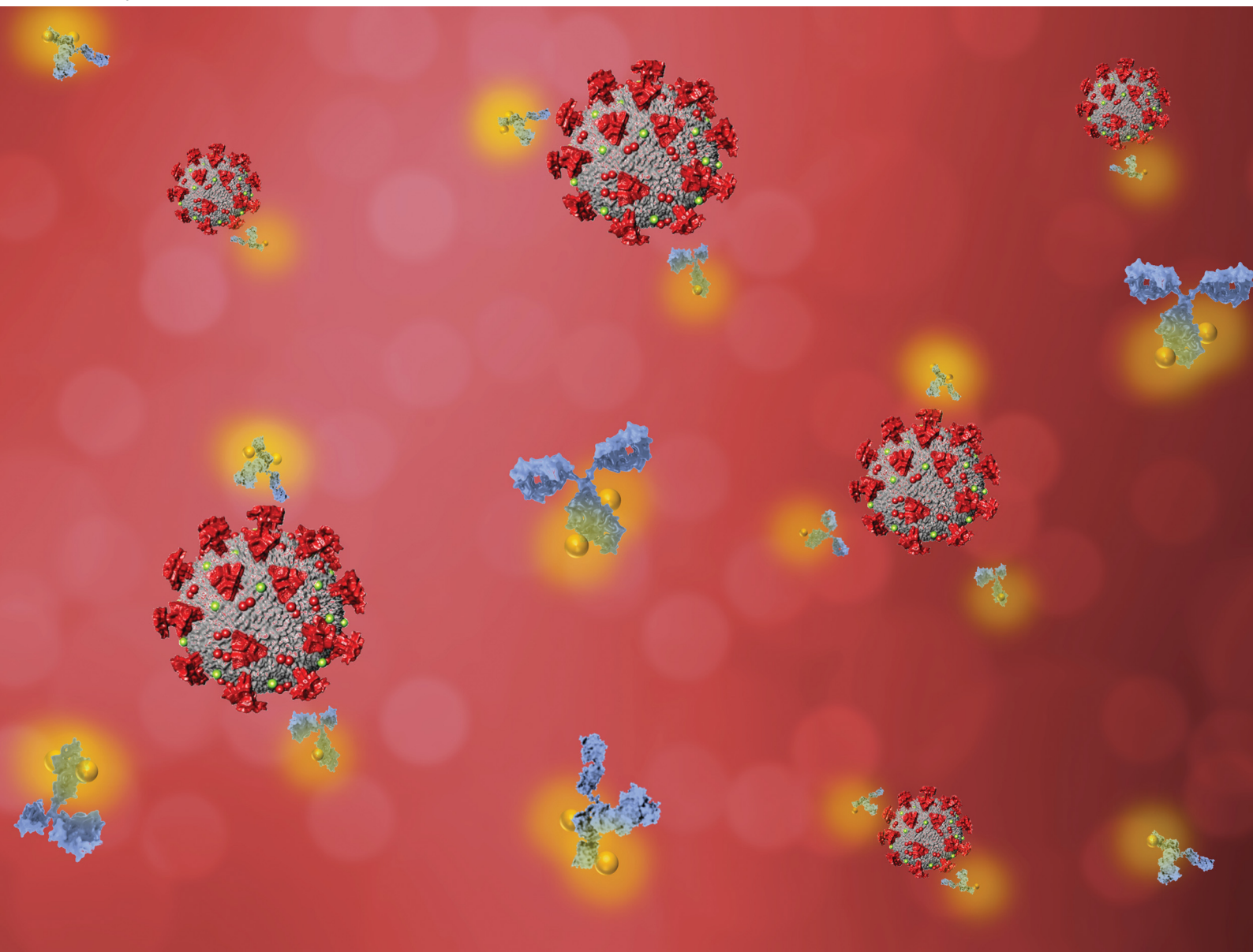


# NJC

New Journal of Chemistry  
rsc.li/njc

A journal for new directions in chemistry



ISSN 1144-0546

**COMMUNICATION**

Antonietta M. Lillo, Rebecca J. Abergel *et al.*  
Development of an actinium-225 radioimmunoconjugate for  
targeted alpha therapy against SARS-CoV-2


Cite this: *New J. Chem.*, 2022, 46, 15795

Received 25th May 2022,  
Accepted 29th June 2022

DOI: 10.1039/d2nj02617a

rsc.li/njc

## Development of an actinium-225 radioimmunoconjugate for targeted alpha therapy against SARS-CoV-2†

Roger M. Pallares,<sup>‡a</sup> Matthew Flick,<sup>a</sup> Katherine M. Shield,<sup>ab</sup> Tyler A. Bailey,<sup>ab</sup> Nileena Velappan,<sup>c</sup> Antonietta M. Lillo\*<sup>c</sup> and Rebecca J. Abergel<sup>ab</sup>

**Targeted alpha therapy offers unique opportunities for the treatment of tumours and infections. Here, we report the development of a new radioimmunoconjugate construct that targets SARS-CoV-2 infected cells, which act as viral reservoirs and promote virus replication and infection spread. The chosen antibody selectively binds to the ACE2-receptor binding domain of the spike protein, and prevents the protein binding to the receptor. Furthermore, the antibody has been radiolabelled with <sup>225</sup>Ac, and the therapeutic performance of the resulting radioimmunoconjugate has been demonstrated *in vitro* against cells mimicking SARS-CoV-2 infection.**

Public awareness of Coronavirus Disease 2019 (COVID-19) first came in late 2019, where early reports of a new pulmonary disease emerged in Wuhan, China.<sup>1,2</sup> SARS-CoV-2, a single stranded ribonucleic acid virus, is the causative agent for the COVID-19 pandemic, which has led to over 2.5 million deaths globally.<sup>1,3</sup> SARS-CoV-2 presents spike glycoproteins on its exterior that bind to specific antigens on the surface of host cells called ACE2 receptors.<sup>4</sup> The high transmissibility of SARS-CoV-2 viral particles expedited its spread on the global scale, resulting in what has become one of the greatest public health crises of the last century, while acting as an impetus for unprecedented biomedical efforts to discover new antiviral therapies. Despite millions of vaccines per day being distributed to the world's population, significantly curbing the spread and severity of COVID-19 cases, effective antivirals are still needed to treat patients with severe symptoms that require

hospitalization. The pandemic continues to highlight the need for drug candidates that are both adaptable to new pathogens and variants, and which can yield biological effectiveness for high-risk patients in need of timely treatment.

Targeted alpha therapy (TAT) is a promising type of radiotherapy currently explored in oncology.<sup>5–7</sup> TAT relies on radioconjugates composed of a targeting vector, such as monoclonal antibodies, covalently bond to bifunctional chelators, which coordinate  $\alpha$ -emitting radionuclides. Because  $\alpha$ -particles display high linear energy transfer and low penetration depth, TAT is able to locally deliver high cytotoxic doses of radiation to tumour cells, while leaving healthy surrounding tissue unaffected. The early success of TAT against several types of cancers has resulted in TAT being proposed as a treatment for other pathologies, such as bacterial and viral infections.<sup>8,9</sup> Because viruses present high radioresistance due to their small size, radiopharmaceuticals usually target infected cells that act as viral reservoirs and facilitate virus replication, rather than targeting the viruses themselves. This antiviral strategy has been effective against HIV-1 in animal models.<sup>10,11</sup> With regards to radionuclide selection, <sup>225</sup>Ac may be preferred over other available  $\alpha$ -emitters because it has a 10-day half-life, which allows for central production and subsequent distribution, and multiple  $\alpha$ -emissions in its decay chain, enhancing the delivered dose.<sup>12</sup> Recently, we developed a set of monoclonal antibodies with high affinity and selectivity for SARS-CoV-2 through *in vitro* evolution of human single-chain antibodies.<sup>13</sup> Although the antibodies were obtained for sensitive and selective point of care detection of SARS-CoV-2, we hypothesized that they could also be used as targeting moieties for TAT against the viral infection.

Here, we show the development of a radioimmunoconjugate for TAT against SARS-CoV-2. The antibody is selective against the spike protein, and can prevent its binding to ACE2 receptor. Our radiolabelling protocol resulted in radiochemical yields between 76 and 87%, while the labeled conjugates retained the antibody native macrostructure integrity. Finally, the potential

<sup>a</sup> Chemical Sciences Division, Lawrence Berkeley National Laboratory, Berkeley, CA, 94720, USA. E-mail: abergel@berkeley.edu

<sup>b</sup> Department of Nuclear Engineering, University of California, Berkeley, CA, 94720, USA

<sup>c</sup> Bioscience Division, Los Alamos National Laboratory, Los Alamos, NM, 87545, USA

† Electronic supplementary information (ESI) available. See DOI: <https://doi.org/10.1039/d2nj02617a>

‡ Current address: Institute for Experimental Molecular Imaging, RWTH Aachen University Hospital, Aachen 52074, Germany.



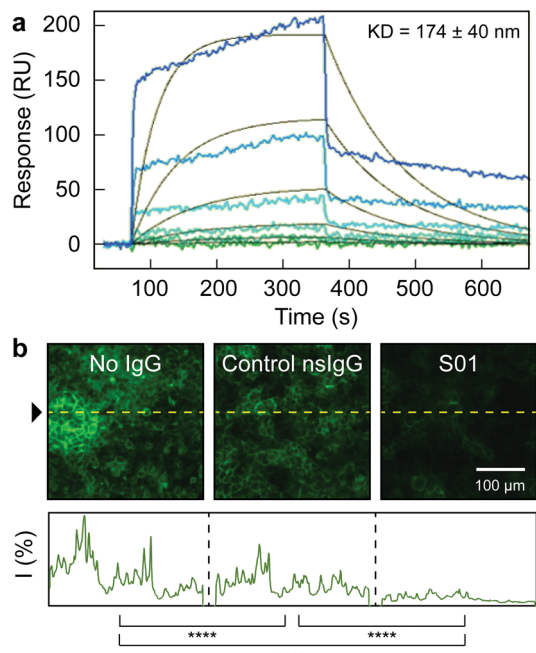


**Fig. 1** (a) Representative sensorgrams of S01-antibody kinetics determined by surface plasmon resonance. S01 concentration ranged from 1.49 (dark green line) up to 500 nM (dark blue line). (b) Confocal microscopy images and luminescence intensity  $I(\%)$  profiles of HEK-293T cells displaying ACE2 after exposure to competing unlabelled antibodies and RBD2-sfGFP. The intensity profiles were measured across the dashed yellow line. (\*\*\*\*) indicates groups that are significantly different with  $p < 0.0001$  (two-tailed unpaired  $t$ -test).

therapeutic performance of the radioimmunoconjugate against SARS-CoV-2 reservoirs was tested with cells displaying spike proteins, which mimicked infected cells.

A monoclonal IgG antibody (S01) was selected as model antibody (Table S1, ESI<sup>†</sup>), since it shows high binding affinity ( $K_d$  of  $170 \pm 40$  nM, Fig. 1a) for the ACE2-receptor binding domain of the spike protein (RBD2). The S01 antibody is a member of a library of unique anti-SARS-CoV-2 antibodies produced by our group, *via* evolution of human single chain antibody libraries, and synergizing phage and yeast display technologies.<sup>13</sup> Moreover, the S01 antibody could also block the binding between the RBD2 and the ACE2 receptor, as demonstrated by competition experiment, where the RBD2 labelled with green fluorescent protein (RBD2-sfGFP) was pre-incubated with the antibody, and later exposed to ACE2-presenting HEK-293T cells. In absence of antibodies or after exposure to a control non-specific IgG (nsIgG), the RBD2-sfGFP could bind to the cells, as observed by confocal microscopy (Fig. 1b). After pre-incubation with S01, however, the RBD2-sfGFP binding to the receptor was mostly prevented. Hence, a radioimmunoconjugate based on S01 antibody, not only would benefit from the radionuclide activity, but also the blocking capabilities of the antibody, as the binding between the spike protein and the ACE2 receptor is an essential step during SARS-CoV-2 infection.

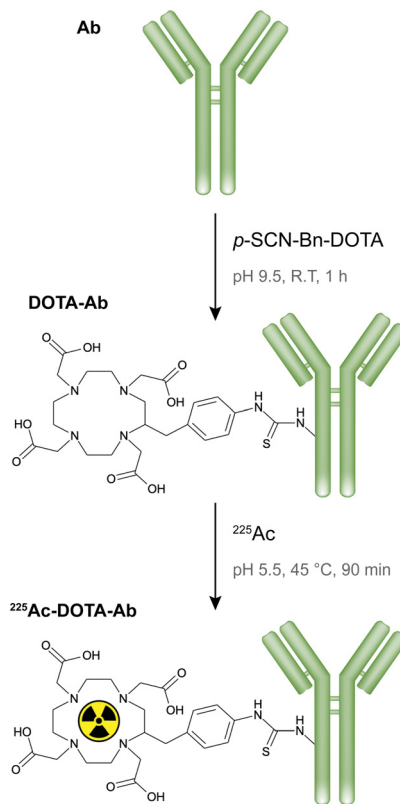


**Fig. 2** Scheme of antibody conjugation with  $p$ -SCN-Bn-DOTA ligand and subsequent radiolabelling with  $^{225}\text{Ac}$ .

Next, DOTA, a macrocyclic chelator commonly utilized to complex  $^{225}\text{Ac}$  in TAT, was coupled to S01 and nsIgG antibodies through lysine-based conjugation, where solvent exposed amine groups of the lysine side chain along the antibodies reacted with  $p$ -SCN-Bn-DOTA to form stable thiourea bonds (Fig. 2). The resulting conjugates retained the antibody native macrostructure integrity as confirmed by polyacrylamide gel electrophoresis (Fig. 3a). The S01 and nsIgG conjugates had a chelator to antibody ratio of 1.6 and 2.2, respectively, as determined by matrix assisted laser desorption ionization-time of flight mass spectrometry (Fig. 3b, for full mass spectra refer to Fig. S1, ESI<sup>†</sup>). The DOTA-antibodies were subsequently radiolabelled with  $^{225}\text{Ac}$  at 45 °C for 90 min following a previously established protocol, which maximizes metal binding, while minimizing protein denaturation.<sup>14–16</sup> The specific activities for the resulting radioimmunoconjugates ( $^{225}\text{Ac}$ -S01 and  $^{225}\text{Ac}$ -nsIgG) were around  $37 \text{ kBq } \mu\text{g}^{-1}$ , as quantified by liquid scintillation counter, and the radiolabelling yield ranged between 75.6 and 86.7% (Table 1). Furthermore, the activities remained quantitatively bound to the constructs as observed by radio thin layer chromatography (Fig. S2, ESI<sup>†</sup>).

Lastly, we decided to evaluate the therapeutic performance of the radioimmunoconjugates *in vitro*. It is worth noting that viruses display high radioresistance,<sup>17</sup> and there are concerns regarding whether they may be missed by alpha and beta radiation due to their small sizes. Nevertheless, successful radioimmunotherapy has been demonstrated against viral



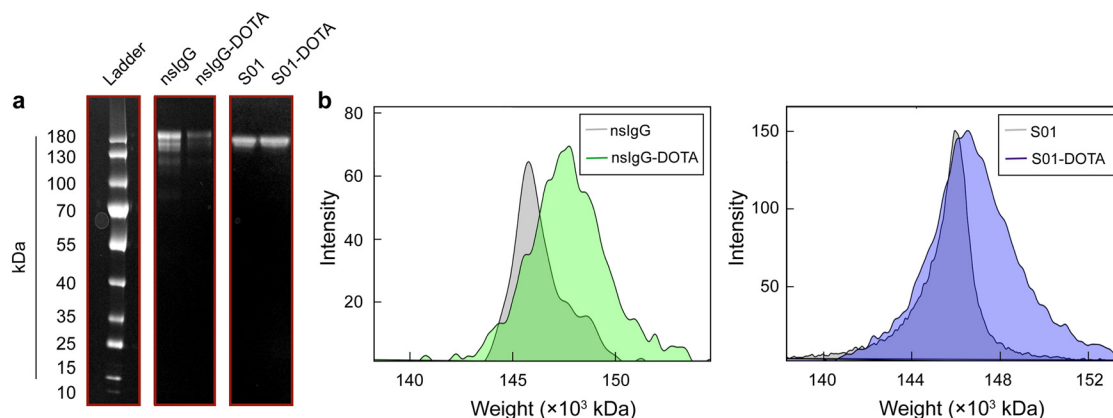


Fig. 3 (a) Gel electrophoresis of antibodies used in the experiment before and after conjugation with DOTA. (b) Mass spectra of nsIgG and S01 antibodies before and after DOTA conjugation.

Table 1 Summary of conjugation and radiolabelling process

|                          | Chelator/<br>antibody | Recovered activity<br>(MBq) | Radiochemical<br>yield (%) |
|--------------------------|-----------------------|-----------------------------|----------------------------|
| $^{225}\text{Ac}$ -S01   | 1.6                   | $4.56 \pm 0.03$             | $75.6 \pm 0.5$             |
| $^{225}\text{Ac}$ -nsIgG | 2.2                   | $5.23 \pm 0.04$             | $86.7 \pm 0.7$             |

Note: 6.03 MBq of  $^{225}\text{Ac}$  were used for the radiolabelling of each radioimmunoconjugate.

infections, such as HIV, in animal models by targeting viral proteins expressed on the surface of infected cells,<sup>10,11</sup> since these cells act as viral reservoirs, where viruses propagate. Similar observations have been reported in cells of COVID-19 patients, where the SARS-CoV-2 infected cells express the spike protein on their surface, which then can interact with ACE2-positive neighbouring cells, causing adverse effects, such as syncytia.<sup>18</sup> Furthermore, it has been reported that SARS-CoV-2 spreads through cell-to-cell transmission.<sup>19</sup> To mimic infected cells, we used HEK-293T cells expressing the SARS-CoV-2 spike glycoproteins. The cells had been transfected with a SARS-CoV-2 spike glycoprotein expression plasmid to provide consistent expression levels of the protein on the cell membrane. Hence, cell viabilities were determined after a 4-day incubation period with the different radioimmunoconjugate treatments (Fig. 4). The half-maximal inhibitory concentration (IC<sub>50</sub>) of  $^{225}\text{Ac}$ -S01 was  $834.9 \pm 18.1$  Bq per well ( $22.6 \pm 0.5$  nCi per well). Furthermore, the antibody did not display observable cytotoxic effects by itself as shown by the consistent cell viability levels after treatment with the unlabelled antibody. Regarding  $^{225}\text{Ac}$ -nsIgG, its IC<sub>50</sub> was 2-fold higher than that of the targeting radioimmunoconjugate, highlighting the benefits of the targeting vector. These results were consistent with a previous publication, which compared the therapeutic effect of targeting and non-targeting antibody-based radiopharmaceuticals for TAT against tumour cells.<sup>14</sup>

In summary, we have developed a new radioimmunoconjugate for potential TAT against SARS-CoV-2 infections.

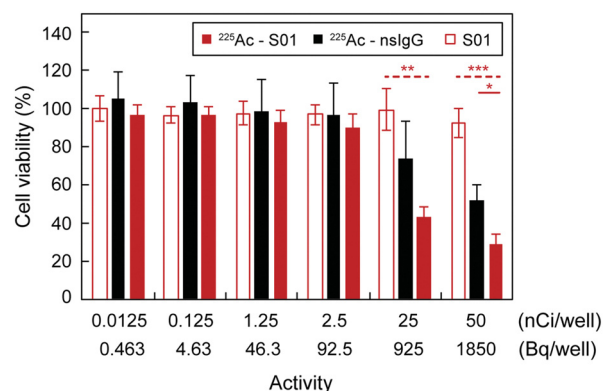


Fig. 4 Cell viability after 4-day incubation times with  $^{225}\text{Ac}$ -S01,  $^{225}\text{Ac}$ -nsIgG, and S01. (\*), (\*\*) and (\*\*\*) indicate groups that are significantly different with  $p < 0.05$ ,  $p < 0.005$  and  $p < 0.001$ , respectively (one-tailed Welch's t-test). The experiments were performed in triplicates, error bars represent one standard deviation of the measurements.

The radioimmunoconjugate is based on an antibody that targets the RBD2 of the spike protein. The antibody itself prevents the binding of RBD2 to the cell ACE2 receptor. We radiolabelled the antibody with  $^{225}\text{Ac}$ , following a protocol developed in-house, which results in a labelling yield between 75.6 and 86.7%. Furthermore, *in vitro* studies showed that the radiopharmaceutical induces cytotoxicity to cells mimicking SARS-CoV-2 infection, which are reported to act as virus reservoirs (promoting virus replication and infection propagation). Combined, all of these results indicate that the proposed radioimmunoconjugate construct could be a potential therapeutic agent for TAT against SARS-CoV-2 infections. It is worth noting, however, that as in the case of TAT against cancer (where TAT is reserved for metastatic patients that are not responding to other forms of therapy), TAT would not be expected to be used to treat the overall population, but only extreme cases. Hence, solely patients with severe infections that are not responding to other treatments would be treated, since TAT has inherent risks (e.g. recoil and release of daughters) that would not justify its use in mild cases.





## Author contributions

R. M. Pallares: conceptualization, methodology, investigation, formal analysis, visualization, writing – original draft. M. Flick: methodology, investigation, writing – review & editing. K. M. Shield: investigation, writing – review & editing. T. A. Bailey: investigation, writing – review & editing. N. Velappan: investigation, resources, writing – review & editing. A. M. Lillo: funding acquisition, conceptualization, methodology, writing – review & editing. R. J. Abergel: funding acquisition, supervision, conceptualization, methodology, writing – review & editing.

## Conflicts of interest

There are no conflicts to declare.

## Acknowledgements

The conjugation, radiolabelling, and targeted alpha-therapy portions of this work were supported by the University of California Contractor Supporting Research Program at Lawrence Berkeley National Laboratory under US Department of Energy Contract No. DE-AC02-05CH11231 (RJA). Initial antibody development was supported by the US Department of Energy (DOE) Office of Science through the National Virtual Biotechnology Laboratory, a consortium of DOE national laboratories focused on response to COVID-19, with funding provided by the Coronavirus CARES Act. The  $^{225}\text{Ac}$  used in this research was supplied by the DOE Isotope Program, managed by the Office of Isotope R&D and Production. The authors acknowledge Dahlia An and Joshua Chen for helpful discussions regarding experimental design, and Drs. Jennifer Wacker and Alyssa Gaiser for their assistance during radiolabelling.

## Notes and references

- 1 J. F.-W. Chan, S. Yuan, K.-H. Kok, K. K.-W. To, H. Chu, J. Yang, F. Xing, J. Liu, C. C.-Y. Yip, R. W.-S. Poon, H.-W. Tsoi, S. K.-F. Lo, K.-H. Chan, V. K.-M. Poon, W.-M. Chan, J. D. Ip, J.-P. Cai, V. C.-C. Cheng, H. Chen, C. K.-M. Hui and K.-Y. Yuen, *Lancet*, 2020, **395**, 514–523.
- 2 A. Remuzzi and G. Remuzzi, *Lancet*, 2020, **395**, 1225–1228.

- 3 Y. M. Bar-On, A. Flamholz, R. Phillips and R. Milo, *eLife*, 2020, **9**, e57309.
- 4 M. A. Tortorici and D. Veesler, in *Advances in Virus Research*, ed. F. A. Rey, Academic Press, 2019, vol. 105, pp. 93–116.
- 5 C. Parker, V. Lewington, N. Shore, C. Kratochwil, M. Levy, O. Lindén, W. Noordzij, J. H. Park and F. Saad, *JAMA Oncol.*, 2018, **4**, 1765–1772.
- 6 J. Kozempel, O. Mokhodoeva and M. Vlk, *Molecules*, 2018, **23**.
- 7 R. M. Pallares, P. Agbo, X. Liu, D. D. An, S. S. Gauny, S. E. Zeltmann, A. M. Minor and R. J. Abergel, *ACS Appl. Mater. Interfaces*, 2020, **12**, 40078–40084.
- 8 E. Dadachova, *J. Med. Imaging Radiat. Sci.*, 2019, **50**, S49–S52.
- 9 R. M. Pallares and R. J. Abergel, *ACS Pharmacol. Transl. Sci.*, 2021, **4**, 1–7.
- 10 E. Dadachova, M. C. Patel, S. Toussi, C. Apostolidis, A. Morgenstern, M. W. Brechbiel, M. K. Gorny, S. Zolla-Pazner, A. Casadevall and H. Goldstein, *PLoS Med.*, 2006, **3**, e427.
- 11 E. Dadachova, S. G. Kitchen, G. Bristol, G. C. Baldwin, E. Revskaya, C. Empig, G. B. Thornton, M. K. Gorny, S. Zolla-Pazner and A. Casadevall, *PLoS One*, 2012, **7**, e31866.
- 12 R. Andrew Kyle Henderson, R. Caterina Fortunata, S. Paul and R. Valery, *Curr. Radiopharm.*, 2018, **11**, 156–172.
- 13 A. M. Lillo, G. S. Waldo, N. Velappan and H. T. B. Nguyen, *US Department of Energy*, 2021, DOI: [10.2172/1760553](https://doi.org/10.2172/1760553).
- 14 A. L. Lakes, D. D. An, S. S. Gauny, C. Ansoborlo, B. H. Liang, J. A. Rees, K. D. McKnight, H. Karsunky and R. J. Abergel, *Mol. Pharmaceutics*, 2020, **17**, 4270–4279.
- 15 M. R. McDevitt, D. Ma, L. T. Lai, J. Simon, P. Borchardt, R. K. Frank, K. Wu, V. Pellegrini, M. J. Curcio, M. Miederer, N. H. Bander and D. A. Scheinberg, *Science*, 2001, **294**, 1537.
- 16 M. Miederer, M. R. McDevitt, G. Sgouros, K. Kramer, N.-K. V. Cheung and D. A. Scheinberg, *J. Nucl. Med.*, 2004, **45**, 129.
- 17 K. S. B. Rose, *J. Environ. Radioact.*, 1992, **15**, 113–133.
- 18 J. Buchrieser, J. Dufloo, M. Hubert, B. Monel, D. Planas, M. M. Rajah, C. Planchais, F. Porrot, F. Guivel-Benhassine, S. Van der Werf, N. Casartelli, H. Mouquet, T. Bruel and O. Schwartz, *EMBO J.*, 2020, **39**, e106267.
- 19 C. Zeng, J. P. Evans, T. King, Y.-M. Zheng, E. M. Oltz, S. P. J. Whelan, L. J. Saif, M. E. Peebles and S.-L. Liu, *Proc. Natl. Acad. Sci. U. S. A.*, 2022, **119**, e2111400119.

